Developments in Soil Science 5B

SOIL CHEMISTRY
B. Physico-Chemical Models

EDITED BY

G.H. BOLT

CONTRIBUTING AUTHORS:

J. BEEK
G.H. BOLT
M.G.M. BRUGGENWERT
F.A.M. DE HAAN
K. HARMSEN
A. KAMPHORST
W.H. VAN RIEMSDIJK

Department of Soil Science and Plant Nutrition, Agricultural University of Wageningen, The Netherlands

R. BRINKMAN

Department of Soil Science and Geology, Agricultural University of Wageningen, The Netherlands

R.W. CLEARY
M.Th. VAN GENUCHTEN

Water Resources Program, Department of Civil Engineering, Princeton University, Princeton, NJ 08540, U.S.A.

A. CREMERS
A. MAES

Faculty of Agronomy, Catholic University of Louvain, Belgium

ELSEVIER SCIENTIFIC PUBLISHING COMPANY
Amsterdam—Oxford—New York 1979

CHAPTER 10

MOVEMENT OF SOLUTES IN SOIL: COMPUTER-SIMULATED AND LABORATORY RESULTS

M. Th. van Genuchten and R.W. Cleary*

Many of the mechanisms which determine the rate at which chemicals move through soil have been discussed in the previous chapter. These mechanisms include such processes as diffusion/dispersion, adsorption, decay, and intra-aggregate diffusion. Exact analytical solutions can be derived for some of these processes, such as for linear adsorption and linear decay (Chapter 9). However, for non-linear cases analytical methods cannot be used to obtain exact solutions of the transport equations and approximate methods must be employed. The use of numerical techniques can provide a useful and often the only alternative in modeling the transport of solutes in such cases. Obviously, numerical and analytical approaches can and should complement and augment each other. For example, an analytical solution may be used to check the accuracy of a numerical program. On the other hand, a numerical solution may be used to demonstrate the appropriateness (or shortcoming) of a particular assumption necessary in the development of an analytical solution.

In this chapter some of the transport equations used at present to describe the movement of chemicals in soils are restated and solutions based on both numerical and analytical techniques are presented. The influence of several mechanisms affecting solute transport phenomena are studied, such as non-linear adsorption, hysteresis in the equilibrium isotherms, and decay. Special consideration is given to the occurrence of non-equilibrium conditions between a given chemical and its adsorbent, the soil.

10.1. MATHEMATICAL DESCRIPTION

The unsteady-state, one-dimensional convective-dispersive mass transport equation which describes the concentration distribution of a chemical undergoing adsorption and linear decay in an unsaturated or saturated soil is given by:

---

* Present address: U.S. Salinity Laboratory, 4500 Glenwood Dr., Riverside, Calif. 92501, U.S.A.

$$\frac{\partial(\theta c)}{\partial t} + \frac{\partial(J^V c)}{\partial x} = \frac{\partial}{\partial x}\left(\theta D \frac{\partial c}{\partial x}\right) - \rho_b \frac{\partial^w q}{\partial t} - k\theta c \qquad (10.1)$$

where c is the solute concentration (ML^{-3}), ^wq is the sorbed concentration ($= q/\rho_b$), ρ_b is the (dry) bulk density of the soil (ML^{-3}), J^V is the Darcy volumetric flux of the feed solution (LT^{-1}), θ is the volumetric moisture content, D is the dispersion coefficient (L^2T^{-1}), k is a first-order rate coefficient (T^{-1}), t is the time (T) and x is the distance (L). The boundary and initial conditions for a semi-infinite system undergoing infiltration with a pulse of water containing a solute of concentration c_f, followed by solute-free water may be stated as:

$$-\theta D \frac{\partial c}{\partial x} + J^V c = \begin{cases} J^V c_f & x = 0 \quad 0 < t \leqslant t_o \\ 0 & x = 0 \quad t > t_o \end{cases}$$

$$\frac{\partial c}{\partial x} = 0 \qquad x \to \infty \qquad t \geqslant 0$$

$$c = 0 \quad \text{in} \qquad 0 \leqslant x < \infty \qquad t = 0 \qquad (10.1a)$$

where t_o is the duration of the solute pulse applied to the soil surface.

If D is assumed constant, (10.1) for steady, saturated conditions (J^V and θ become constants), or for unsaturated, constant moisture content conditions (Warrick et al., 1971), reduces to:

$$\frac{\partial c}{\partial t} + v \frac{\partial c}{\partial x} = D \frac{\partial^2 c}{\partial x^2} - \frac{\rho_b}{\theta} \frac{\partial^w q}{\partial t} - kc \qquad (10.2)$$

and the boundary and initial conditions become:

$$-D \frac{\partial c}{\partial x} + vc = \begin{cases} vc_f & x = 0 \quad 0 < t \leqslant t_o \\ 0 & x = 0 \quad t > t_o \end{cases}$$

$$\frac{\partial c}{\partial x} = 0 \qquad x \to \infty \qquad t \geqslant 0$$

$$c = 0 \quad \text{in} \qquad 0 \leqslant x < \infty \qquad t = 0 \qquad (10.2a)$$

where v is the average interstitial or pore-water velocity ($v = J^V/\theta$).

Solutions of (10.2) can be obtained after specifying the adsorption rate $\partial^w q/\partial t$ in the transport equation. Several models for adsorption or ion exchange may be used for this purpose. These may be divided into two broad categories: equilibrium models which assume instantaneous adsorption of the chemical, and kinetic models which consider the rate of approach towards equilibrium. Table 10.1 presents examples of some of the adsorption models at present available. Not included in table 10.1 are those models

TABLE 10.1.

Some equations available to describe the adsorption of chemical on soil

Model	Equation	Reference
1. Equilibrium		
1.1 (linear)	$^{w}q = k_1 c + k_2$	Lapidus and Amundson (1952) Lindstrom et al. (1967)
1.2 (Langmuir)	$^{w}q = \frac{k_1 c}{1 + k_2 c}$	Tanji (1970) Ballaux and Peaslee (1975)
1.3 (Freundlich)	$^{w}q = k_1 c^{k_2}$	Lindstrom and Boersma (1970) Swanson and Dutt (1973)
1.4	$^{w}q = k_1 c \exp(-2k_2 {}^{w}q)$	Lindstrom et al. (1971) Van Genuchten et al. (1974)
1.5 (modified Kielland)	$^{w}q/{}^{w}q_f = c[c + k_1(c_f - c) \exp\{k_2(c_f - 2c)\}]^{-1}$	Lai and Jurinak (1971)
2. Non-equilibrium		
2.1 (linear)	$\frac{\partial {}^{w}q}{\partial t} = k_r(k_1 c + k_2 - {}^{w}q)$	Lapidus and Amundson (1952) Oddson et al. (1970)
2.2 (Langmuir)	$\frac{\partial {}^{w}q}{\partial t} = k_r\left(\frac{k_1 c}{1 + k_2 c} - {}^{w}q\right)$	Hendricks (1972)
2.3 (Freundlich)	$\frac{\partial {}^{w}q}{\partial t} = k_r(k_1 c^{k_2} - {}^{w}q)$	Hornsby and Davidson (1973) Van Genuchten et al. (1974)
2.4	$\frac{\partial {}^{w}q}{\partial t} = k_r \exp(k_2 {}^{w}q)\{k_1 c \exp(-2k_2 {}^{w}q) - {}^{w}q\}$	Lindstrom et al. (1971)
2.5	$\frac{\partial {}^{w}q}{\partial t} = k_r({}^{w}q_f - {}^{w}q) \sinh\left(k_1 \frac{{}^{w}q_f - {}^{w}q}{{}^{w}q_f - {}^{w}q_i}\right)$	Fava and Eyring (1956) Leenheer and Ahlrichs (1971)
2.6	$\frac{\partial {}^{w}q}{\partial t} = k_r(c)^{k_1}({}^{w}q)^{k_2}$	Enfield et al. (1976)

which describe the competition between two ionic species, such as the commonly used cation exchange equations. Except for a few cases (cf. Lai and Jurinak, 1971), generally two transport equations (i.e. of the type given by (10.1)) have to be solved for such multi-ion problems. Only single-ion transport models will be considered here.

Most of the equilibrium models listed in Table 10.1 are special cases of the non-equilibrium models. Model 1.4 in particular follows directly from the rate equation used by Lindstrom et al. (1971) (model 2.4) by setting the time derivative, $\partial^w q/\partial t$, to zero. All adsorption models further represent reversible adsorption reactions, except for model. 2.6. The rate equation proposed by Enfield et al. (1976) is an irreversible adsorption equation because it does not allow for any chemical desorption (the adsorption rate is always positive). Model 2.6 was used by Enfield et al. to describe the adsorption of phosphorus on several soils.

For illustrative purposes this chapter will consider only models 1.3 and 2.3, i.e. the Freundlich-type equilibrium and non-equilibrium adsorption equations. Both models will be discussed separately.

10.2. EQUILIBRIUM ADSORPTION

It has been shown by several authors (cf. Kay and Elrick, 1967; Bailey et al., 1968; Davidson and Chang, 1972) that for many organic chemicals the relationship, at equilibrium, between adsorbed (^{w}q) and solution concentration (c) can be described by a general Freundlich isotherm (model 1.3):

$$^w q = kc^n \tag{10.3}$$

where k and n are temperature-dependent constants. Although (10.3) could be derived on physicochemical grounds (cf. Rideal, 1930), it suffices for the present objective to treat k and n as just empirical constants which may be determined experimentally, for example using batch equilibration methods.

Equation (10.3) assumes that once the chemical and the porous matrix are brought sufficiently close together, adsorption will be an instantaneous process. However, the equation does not specify the exact mode in which the chemical and the soil adsorption sites may be brought together (e.g. convective transport, diffusion, a shaking process, etc.).

Equation (10.3) may be differentiated with respect to time and substituted into (10.2). This allows the transport equation to be written in terms of one dependent variable, c:

$$\frac{\partial c}{\partial t} = \frac{1}{R_f}\left(D\frac{\partial^2 c}{\partial x^2} - v\frac{\partial c}{\partial x} - kc\right) \tag{10.4}$$

where the retardation factor R_f (introduced by Hashimoto et al., 1964) is defined as:

$$R_f \equiv 1 + q'/\theta \quad \text{(cf. (9.7) and (9.9))}$$

$$= 1 + \rho_b n k c^{n-1}/\theta \tag{10.5}$$

The retardation factor defines the mean velocity of the moving liquid relative to the mean velocity at which the chemical itself moves through the soil.

Exact analytical solutions of (10.4) are available only when a linear adsorption isotherm is present ($n = 1$). The retardation factor then becomes independent of the solute concentration, i.e.:

$$R_f = 1 + \rho_b k/\theta \tag{10.5a}$$

The solution of (10.4) subject to a first-type boundary condition at the soil surface and for a semi-infinite profile has been given in Gershon and Nir (1969). Cleary and Adrian (1973) derived the analytical solution for the case of a finite profile with linear adsorption and a first-type boundary condition. Selim and Mansell (1976) extended Cleary and Adrian's work by including the effects of linear decay. The direct solution of (10.4) subject to the initial and third-type boundary conditions given by (10.2a) is apparently not in the literature. Without giving the lengthy integral transform derivation, we present this solution for the first time here:

$$\frac{c}{c_f} = \begin{cases} c_1(x,t) & 0 < t \leqslant t_0 \\ c_1(x,t) - c_1(x, t-t_0) & t > t_0 \end{cases} \tag{10.6}$$

where:

$$\begin{aligned} c_1(x,t) = {} & \frac{v}{v_\iota} \exp(vx/2D) \left[\exp(-v_\iota x/2D)\, \operatorname{erfc} \left\{ \frac{R_f x - v_\iota t}{(4DR_f t)^{1/2}} \right\} \right. \\ & \left. - \exp(v_\iota x/2D)\, \operatorname{erfc} \left\{ \frac{R_f x + v_\iota t}{(4DR_f t)^{1/2}} \right\} \right] \\ & + \frac{v^2}{4kD} \exp(vx/D) \left[2 \exp(-kt/R_f)\, \operatorname{erfc} \left\{ \frac{R_f x + vt}{(4DR_f t)^{1/2}} \right\} \right. \\ & + \left(\frac{v}{v_\iota} - 1 \right) \exp\left\{ -\frac{x}{2D}(v + v_\iota) \right\} \operatorname{erfc} \left\{ \frac{R_f x - v_\iota t}{(4DR_f t)^{1/2}} \right\} \\ & \left. - \left(\frac{v}{v_\iota} + 1 \right) \exp\left\{ -\frac{x}{2D}(v - v_\iota) \right\} \operatorname{erfc} \left\{ \frac{R_f x + v_\iota t}{(4DR_f t)^{1/2}} \right\} \right] \end{aligned} \tag{10.7}$$

and:

$$v_\iota = v\sqrt{1 + 4kD/v^2}$$

Equation (10.7) may be simplified for the particular case when no decay processes are present ($k = 0$). By applying L'Hospital's rule to the second term of (10.7) it may be shown that the equation reduces to the solution derived by Lindstrom et al. (1967) for no decay:

$$c_1(x,t) = \frac{1}{2}\operatorname{erfc}\left\{\frac{R_f x - vt}{(4DR_f t)^{1/2}}\right\} + \left(\frac{v^2 t}{\pi D R_f}\right)^{1/2} \exp\left\{-\frac{(R_f x - vt)^2}{4DR_f t}\right\}$$

$$-\frac{1}{2}\exp(vx/D)\left(1 + \frac{vx}{D} + \frac{v^2 t}{DR_f}\right)\operatorname{erfc}\left\{\frac{R_f x + vt}{(4DR_f t)^{1/2}}\right\} \qquad (10.8)$$

Referring to section 9.7 of the previous chapter it is pointed out that in the above equation (10.7) the decay-diffusion/dispersion interaction is expressed in terms of the variable $v_\iota = v(1 + \iota)$, whereas previously the parameter ι was used for this purpose (cf. (9.105)). Since the present case is based on a linear adsorption isotherm, the retardation factor R_f is a constant, so that $v/R_f = v^*$ and $D/R_f = D^*$ (9.104). Formulating (10.7) in terms of the variables used previously:

$$L_D = D/v = D^*/v^*$$

$$\xi = \tfrac{1}{2}(x - v^*t)/\sqrt{D^*t}; \qquad \xi_\iota = \tfrac{1}{2}\{x - (\iota + 1)v^*t\}/\sqrt{D^*t}$$

$$\alpha = v^*t/\sqrt{D^*t}; \qquad \alpha_\iota = (\iota + 1)v^*t/\sqrt{D^*t}$$

one obtains:

$$\frac{c}{c_f} = \frac{\exp(-\frac{1}{2}\iota x/L_D)}{(\iota + 2)}\left[\operatorname{erfc}(\xi_\iota) - \exp\{(\iota + 1)x/L_D\}\operatorname{erfc}(\xi_\iota + \alpha)\right]$$

$$+\frac{2\exp(x/L_D)}{\iota(\iota + 2)}\left[\exp\{-\tfrac{1}{4}\iota(\iota + 2)\alpha^2\}\operatorname{erfc}(\xi + \alpha)\right.$$

$$\left.-\exp(\tfrac{1}{2}\iota x/L_D)\operatorname{erfc}(\xi_\iota + \alpha_\iota)\right] \qquad (10.7a)$$

where $x/L_D \equiv (\xi + \alpha)^2 - \xi^2$ has been left intact. For $\iota \to 0$, $\xi_\iota \to \xi$, and $\alpha_\iota \to \alpha$; expanding the last term to cancel ι appearing in the denominator then leads immediately to the previous equation (9.56), which is thus identical with (10.8) above.

Unfortunately, no exact analytical solutions are available when the adsorption isotherm is non-linear. Approximate solutions may still be derived for some special cases as was shown in chapter 9 for favorable exchange ($n < 1$). Generally, however, one must resort to numerical techniques in order to obtain results (Van Genuchten and Wierenga, 1974; Gupta and Greenkorn, 1976). The numerical solutions presented in this chapter were obtained using a finite difference approach, and were programmed in the

IBM S/360 CSMP-language as discussed extensively elsewhere (Van Genuchten and Wierenga, 1974, 1976a). In the CSMP approach, the spatial derivatives are approximated with suitable finite differences, while the integration in time is performed using a predictor–corrector Runge-Kutta type algorithm (IBM, 1967). This approach has proven to be a relatively simple way of obtaining solutions for rather complex distributive systems, without sacrificing accuracy in the results.

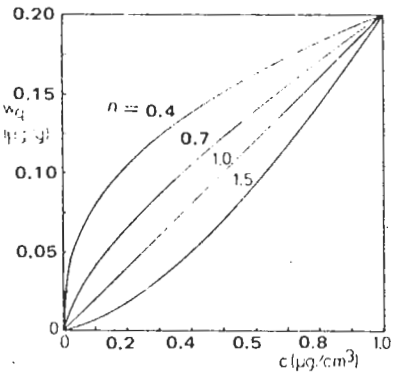

Fig. 10.1. Freundlich equilibrium plots for k = 0.2 and four different values for the exponent n.

10.2.1. Non-linear adsorption effects

First the influence of a non-linear adsorption isotherm on the shape and position of a solute pulse travelling through a soil column will be studied. For illustrative purposes the constant k in (10.3) was chosen to be 0.2 and the value of n was allowed to vary between 0.4 and 1.5, as shown in Fig. 10.1. The isotherms are clearly much more non-linear near the origin, but become approximately linear as the maximum value is approached. The maximum concentration, c_f, of the feed solution was given an arbitrary value of 1.0 $\mu g/cm^3$. The curves plotted in Fig. 10.1 were subsequently used in conjunction with (10.4) ($k = 0$) to calculate the distribution of the chemical versus depth, both in the solution and adsorbed phases. Results are shown in Fig. 10.2. A total of 20 cm^3 of a chemical solution was applied to the soil surface and leached out with a solute-free solution at a rate (J^V) of 16 cm/day. The chemical hence is in the feed solution for only 1.25 days (t_0). The calculated profiles in Fig. 10.2 are plotted after three days. Other data used to calculate the curves are given with Fig. 10.2.

Recalling the extensive discussion on the shape of the "base front", i.e. the front in the absence of diffusion/dispersion, as influenced by concave, linear, and convex adsorption isotherms (see section 9.3), one finds that the curves based on the linear isotherm ($n = 1$) exhibit a nearly symmetrical

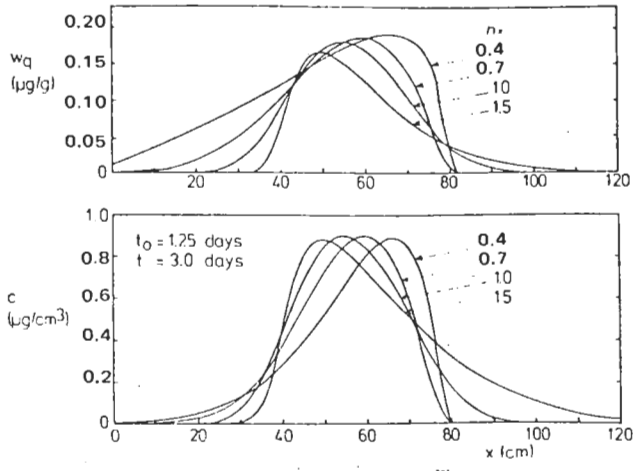

Fig. 10.2. Solution (c) and adsorbed (^{w}q) concentration distributions versus distance as obtained with the four equilibrium isotherms of Fig. 10.1, and the following soil-physical data: $\rho_b = 1.40\ g/cm^3$, $J^V = 16\ cm/day$, $\theta = 0.40\ cm^3/cm^3$ and $D = 30\ cm^2/day$.

shape for the present block feed, i.e. a block front as modified by diffusion/dispersion. This is not true, however, when n deviates from one: the more non-linear the adsorption isotherm, the more asymmetrical the resulting solute distribution becomes. When $n = 0.4$, for example, a very steep solute front develops while the distribution near the soil surface becomes much more dispersed. The appearance of a sharp front may be explained by considering the ratio v/R_f in (10.4). Since R_f increases rapidly with decreasing concentration ($n = 0.4$), the ratio v/R_f will decrease when the solute concentration becomes smaller, i.e. ahead of the solute front. This in turn slows down the movement of the chemical before the front. The ratio v/R_f on the other hand is much higher at the higher concentrations. The higher the concentration, the faster the apparent velocity of the chemical will be; the higher concentrations now tend to override the lower concentrations and a step front will develop. Owing to the developing high concentration gradients, however, the front will never attain a block form. The diffusion forces become very strong here and will always maintain a smooth curve. It should be noted that the retardation factor also influences the steepness of the front through the ratio D/R_f in (10.4). Since R_f is very large near the toe of the concentration front, the apparent dispersion of the solute distribution will be much less here than at the higher concentration (cf. the relevant discussion on p.321 in the previous chapter).

The sharpening of the solute front when $n < 1$ may also be explained by considering the differential capacity for adsorption, d^wq/dc, i.e. the slope of the equilibrium isotherms. When $n < 1$, d^wq/dc is relatively large at the lower concentrations. This means that the rate of adsorption at lower concentrations is much higher than at higher concentrations. Because more material

will be drawn from the soil solution towards the adsorption sites located at the downstream side of the solute front, the solution concentration initially will increase only very slowly. With each increase in concentration, however, $d^w q/dc$ decreases, resulting in the adsorption rate becoming smaller. This in turn forces the solution concentration to increase faster, leading to the observed steep front. When the bulk of the chemical has passed, i.e. near the soil surface, a small decrease in concentration initially will result in the release of only a small amount of material adsorbed ($d^w q/dc$ is small at the higher concentrations). With each decrease in concentration, the desorption rate of the chemical increases, bringing more and more chemical into solution and hence resulting in a slower decrease in the solution concentration. This then explains the highly dispersed solute distributions near the entrance of the soil column.

When $n > 1$, the reverse occurs. Adsorption at the lower concentrations is now relatively minor and the toe of the front propagates with a velocity nearly equal to that of the liquid. At the higher concentration, however, adsorption is now much more extensive, resulting in a slower rate of movement. Hence the concentration front becomes increasingly more dispersed in appearance as time progresses. After most of the chemical has passed and the concentration starts decreasing, initially much of the chemical which was adsorbed will go into solution ($d^w q/dc$ is large) and hence the concentration will remain relatively high. Again, with each decrease in concentration, less material will go into solution ($d^w q/dc$ decreases rapidly) and the solution concentration will drop quicker, resulting in the steep front upstream of the solute pulse. Some of these observations have also been discussed in the previous chapter. The curves presented in Fig. 10.2 are representative of the processes of desodication ($n < 1$) and sodication ($n > 1$), although the adsorption isotherms may be somewhat different than the Freundlich ones used here (cf. sections A7.3.3 and A7.4 in volume A of this text, and the discussion of Figs. 9.11 and 9.14).

10.2.2. Chemical hysteresis effects

Several studies recently have revealed the possibility of a hysteresis phenomenon when studying the adsorption and desorption of different pesticides and soils. Hornsby and Davidson (1973), Swanson and Dutt (1973), and Van Genuchten et al. (1974) all encountered hysteresis in the equilibrium isotherms. In these studies the coefficients k and n in the Freundlich isotherm (10.3) were found to depend on the sorption direction, i.e. whether *ad*sorption ($\partial^w q/\partial t > 0$) or *de*sorption ($\partial^w q/\partial t < 0$) occurred. Figure 10.3 shows an example where adsorption and desorption follow different curves. These isotherms were used by Van Genuchten et al. (1974) to describe the movement of the herbicide picloram (4-amino-3,4,6-trichloropicolinic acid) through a Norge loam soil. Other examples of

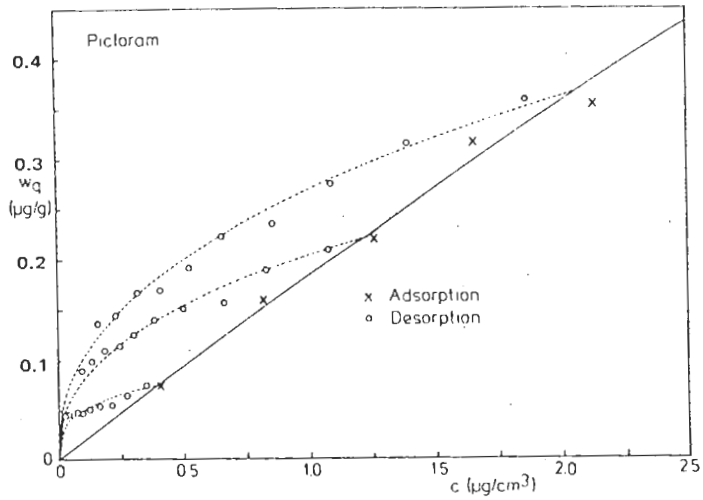

Fig. 10.3. Equilibrium adsorption ($^{w}q_a$) and desorption ($^{w}q_d$) isotherms for Picloram sorption on Norge loam. The adsorption isotherm is given by $^{w}q_a = 0.180\ c^{0.94}$. The desorption isotherms may be calculated from equations 10.10 and 10.11.

hysteresis can be found in the studies quoted above. The desorption parameters of the curves plotted in Fig. 10.3 may be determined by equating the Freundlich equations for adsorption and desorption, as follows:

$$^{w}q_r = k_a(c_r)^{n_a} = k_d(c_r)^{n_d} \tag{10.9}$$

where the subscripts a and d refer to adsorption and desorption, respectively, and where c_r and $^{w}q_r$ represent the solution and sorbed concentrations when the sorption direction is reversed from adsorption to desorption, i.e. where $\partial^{w}q/\partial t = 0$. Solving (10.9) for k_d yields:

$$k_d = {}^{w}q_r \left\{\frac{k_a}{{}^{w}q_r}\right\}^{n_d/n_a} \tag{10.10}$$

The ratio n_a/n_d was found to be a function of $^{w}q_r$:

$$n_a/n_d = 2.105 + 0.062\,{}^{w}q_r^{-1.076} \tag{10.11}$$

For the three curves shown in Fig. 10.3 the values of n_a/n_d are 2.22 ($^{w}q_r$ = 0.365), 2.34 ($^{w}q_r = 0.223$) and 2.98 ($^{w}q_r = 0.0767$). These values are close to those reported by Swanson and Dutt (1973), who observed an average value of 2.3 for the adsorption and desorption of atrazine using different soils. Similar values were obtained also by Hornsby and Davidson (1973), and Van Genuchten et al. (1977). Smaller values, however, were obtained by Wood and Davidson (1975), and Farmer and Aochi (1974) for the desorption of different organic chemicals from different soils.

The isotherms shown in Fig. 10.3 were used by Van Genuchten et al. (1974) to calculate effluent concentration distributions of picloram from 30-cm long columns. Results for one experiment (fig. 3 in the original study) are shown in Fig. 10.4 and are compared with the experimental effluent data. The concentrations in the Figure are plotted versus the number of pore volumes leached through the soil column.

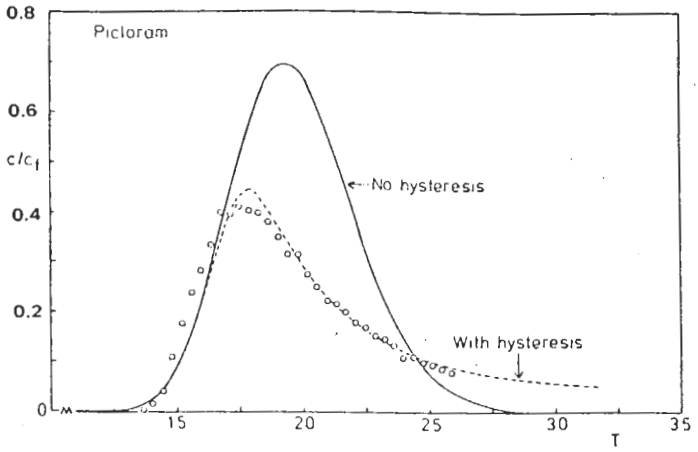

Fig. 10.4. Calculated and observed effluent curves for Picloram movement through Norge loam. The calculated curves were obtained with the following soil-physical data: ρ_b = 1.53 g/cm^3, J^V = 14.2 cm/day, θ = 0.363 cm^3/cm^3, D = 2.8 cm^2/day, t_0 = 0.896 days (T_0 = 1.17) and L = 30 cm.

The number of pore volumes may be defined as the amount of liquid leached through the column, divided by the liquid capacity of the column, i.e.:

$$T \equiv \frac{J^V t}{\theta L} = \frac{vt}{L} \qquad (10.12)$$

where L is the length of the column. When no adsorption occurs and diffusion/dispersion processes are neglected, the solute in the column would travel with a velocity equal to that of the liquid in which it is dissolved. The retardation factor R_f in that case would be 1.0 and the chemical will appear in the effluent after exactly one pore volume. When adsorption occurs, however, the chemical will travel slower than the liquid and hence will appear in the effluent after more than one pore volume of solution is leached through the soil column. Assuming a linear approximation of the *ad*sorption isotherm (k_a = 0.18, n_a = 1.0), and using the data of Fig. 10.4, one may calculate a retardation factor R_f of 1.76 ((10.5a)). The chemical will now travel with a mean velocity equal to $(1.76)^{-1}$ or 0.57-times the velocity of the liquid, i.e. the chemical will appear in the effluent after 1.76 pore volumes. Owing to the presence of diffusion and dispersion processes and the slight non-linear character of the adsorption isotherm, the exact break-through of the chemical may be somewhat different, but should still be centered around 1.76 pore volumes (Fig. 10.4). By plotting the relative concentration versus pore volumes, the adsorption characteristics of the chemical and the soil are more clearly shown.

Figure 10.4 illustrates the importance of using both adsorption and desorption characteristics. The solid line is calculated when the hysteresis phenomena are ignored and adsorption and desorption are assumed to follow the same (adsorption) isotherm. The effluent curve in this case acquires a fairly symmetrical shape. When hysteresis is included in the calculations a much better description of the data results. The front side of the calculated curves is not affected by hysteresis, since the chemical processes are determined here by the *ad*sorption isotherm only. During desorption, however, the isotherm is convex upwards ($n < 1$) and a long "tail" develops during elution of the chemical. The development of the tailing in Fig. 10.4 may be explained in a similar way as was done in the previous section for a general non-linear isotherm, which resulted in the dispersed appearance of the chemical near the entrance of the soil column (Fig. 10.2, $n = 0.4$).

Figure 10.4 not only shows that the occurrence of hysteresis in the equilibrium isotherms induces heavy tailing, but also that the peak concentration decreases significantly. From the Figure it is clear that excluding hysteresis effects when calculating effluent concentration distributions may result in serious disagreements between observed and calculated distributions.

10.2.3. Decay effects

The two previous examples were obtained with the assumption that the chemical undergoes no decay reactions (biological or chemical transformation). In many systems which contain such compounds as pesticides, ammoniacal fertilizers, and radioactive materials, decay processes are usually present. A thorough analytical analysis of decay was given in section 9.7, and only one example will be briefly discussed here.

To illustrate the influence of a decay sink on an effluent curve, the experimental parameters of the last example were used (assuming no hysteresis), together with a first-order decay coefficient k (cf. (10.2)) which was allowed to vary between 0.0 and 0.5 day^{-1}. Results were obtained for both a short pulse ($t_0 = 0.896$ day) and a continuous feed solution, the latter case resulting in a complete break-through of the chemical (Fig. 10.5; solid and dashed lines, respectively). Owing to the increase in degradation with increasing values of k, the maximum concentration in the effluent clearly decreases. The complete break-through curves (dashed lines) approach an equilibrium value which depends on the value of k used in the calculations. It should be noted that a slightly non-linear isotherm was used to obtain the curves plotted in Fig. 10.5 ($n = 0.94$). When the isotherm is approximated by a linear relation ($k = 0.18$, $n = 1.0$), the concentration distributions are given exactly by the analytical solution of (10.7). The steady-state value of the concentration during break-through (Fig. 10.5) for this case is given by (see for example Gershon and Nir, 1969):

$$\frac{c}{c_f} = \frac{2 \exp\left\{\frac{vx}{2D}\left(1 - \sqrt{1 + 4Dk/v^2}\right)\right\}}{\left(1 + \sqrt{1 + 4Dk/v^2}\right)} \tag{10.13}$$

$$\left(= \frac{2 \exp\left(-\tfrac{1}{2} v\iota x/D\right)}{(\iota + 2)}\,;\ \text{cf. (9.107)}\right) \tag{10.14}$$

It is interesting to note that this steady-state solution ($\partial c/\partial t = \partial {}^{w}q/\partial t = 0$) holds regardless of whether or not the chemical is adsorbed by the medium, and hence is independent of the particular form of the adsorption isotherm. The final concentrations in Fig. 10.5, reached after approximately 2.3 pore volumes, can, therefore, also be calculated with (10.13).

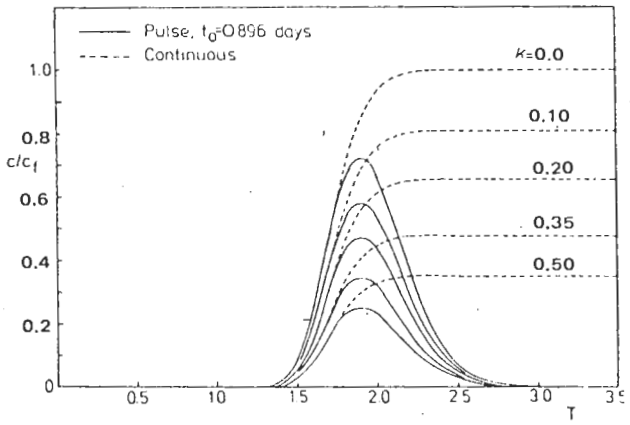

Fig. 10.5. Effect of first-order decay on Picloram movement through Norge loam. The soil-physical data are the same as used in Fig. 10.4.

10.3. NON-EQUILIBRIUM ADSORPTION

In Fig. 10.4 experimental effluent concentrations were compared with calculated curves which were obtained with the assumption that at any time equilibrium exists between sorbed (^{w}q) and solution (c) concentrations. Although an excellent description of the experimental data was obtained, provided the observed hysteresis phenomenon was included in the numerical calculations, some small deviations are apparent at the break-through side of the effluent curves. The chemical seems to travel somewhat faster than predicted with the equilibrium model. Similar and more severe deviations between experimental and equilibrium curves have been observed in a number of studies (Kay and Elrick, 1967; Davidson and Chang, 1972; Green et al., 1972; Van Genuchten et al., 1974, 1977; Wood and Davidson, 1975).

The deviations mentioned here are presumably caused by the inability of the chemical to be adsorbed instantaneously by the medium during its transport through the soil.

Many explanations have been given to account for this inability to reach equilibrium. First there is the possibility that a true kinetic adsorption mechanism is present, i.e. the chemical will be adsorbed slowly, even when it is assured that the chemical molecule and soil adsorption site are physically in close contact. Hence a finite rate of adsorption is present. When this is the case and it is the only reason for non-equilibrium, the movement of the chemical in a soil should be described completely by coupling the transport equation (10.2) with one of the kinetic rate equations listed in Table 10.1 (or with any other appropriate rate equation).

A second possible reason for non-equilibrium may be the significant physical resistances encountered by a chemical in trying to reach the sorption sites of the porous matrix during its movement through the soil. This may be especially true for aggregated (Green et al., 1972) and/or unsaturated soils (Nielsen and Biggar, 1961). In these cases the chemical has to diffuse first out of the larger, liquid-filled pores (mobile liquid) into an immobile liquid region before it can be adsorbed by those sorption sites located inside the aggregates or along the walls of blind pores. This situation is now merely a physical problem in that the physical make-up of the medium is responsible for non-equilibrium (*physical* vs. *kinetic* non-equilibrium). Adsorption in the immobile region of the soil becomes now a diffusion-controlled mechanism. It should be noted that this physical non-equilibrium may be demonstrated also with chemicals which are not adsorbed by the medium. Material still has to diffuse into the immobile zone, especially when the soil is highly aggregated (see for example the studies by Nielsen and Biggar, 1961; McMahon and Thomas, 1974; Van de Pol, 1974). Both mechanisms for non-equilibrium will now be discussed separately.

10.3.1. Kinetic non-equilibrium

As mentioned previously, serious deviations have been observed between experimental data and predictions based on equilibrium models. Figure 10.6 shows an example of how serious these deviations can be. The example is taken from Van Genuchten et al. (1977), who studied the adsorption and movement of the herbicide 2,4,5-T (2,4,5-Trichlorophenoxyacetic acid) through 30-cm long columns containing Glendale clay loam soil. The equilibrium adsorption and desorption isotherms for this herbicide and soil are given in Fig. 10.7. Note again the hysteresis between adsorption and desorption. The isotherms, both for adsorption and desorption, are described with Freundlich-type equations. The ratio n_a/n_d was found to be 2.3 ((10.10)), resulting in desorption curves of the form:

$$^{w}q = k_d c^{0.344} \qquad (10.15)$$

The curves plotted in Fig. 10.6 were obtained with and without the inclusion of hysteresis effects in the calculations. Once again one can see that the elution side of the experimental effluent curve is reasonably well described when hysteresis is taken into account. The break-through part of the effluent curve, however, is poorly predicted.

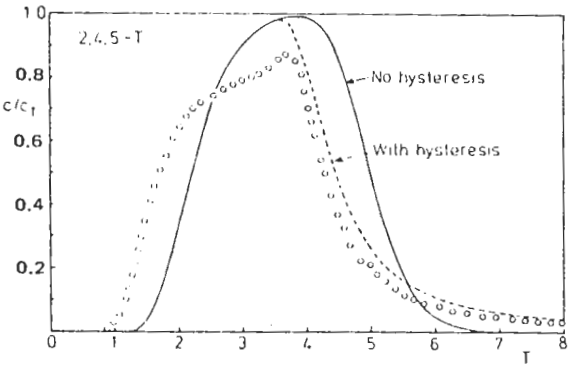

Fig. 10.6. Calculated and observed effluent curves for 2,4,5-T movement through Glendale clay loam. The following soil-physical data were used in the calculations: $\rho_b = 1.36$ g/cm^3, $J^V = 5.11$ cm/day, $\theta = 0.473$ cm^3/cm^3, $T_0 = 2.761$, $D = 8.4$ cm^2/day and $L = 30$ cm.

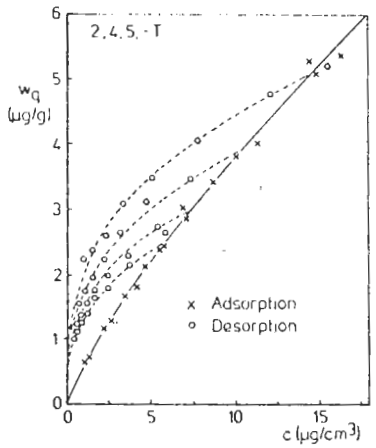

Fig. 10.7. Equilibrium adsorption ($^{w}q_a$) and desorption ($^{w}q_d$) isotherms for 2,4,5-T sorption on Glendale clay loam. The adsorption isotherm is given by $^{w}q_a = 0.616\, c^{0.792}$, the desorption curves by $^{w}q_d = k_d c^{0.344}$.

Several authors have suggested the use of a kinetic model, rather than an equilibrium one, to improve the predictions. A rate equation frequently used

is based on model 2.3 (Table 10.1). In the present notation, this equation may be written as:

$$\frac{\partial {}^{w}q}{\partial t} = k_r(kc^n - {}^{w}q) \tag{10.16}$$

where k_r is a kinetic rate coefficient with units of day^{-1}. Several analytical solutions of (10.2) and (10.16) may be derived, provided the adsorption isotherm is linear ($n = 1$) and hysteresis is neglected (Van Genuchten, 1974, appendix B). Subject to the particular initial and boundary conditions of (10.2a), the solution may be expressed in the following dimensionless form:

$$\frac{c}{c_f} = \begin{cases} c_1(s, t) & 0 < t \leqslant t_0 \\ c_1(s, t) - c_1(s, t - t_0) & t > t_0 \end{cases} \tag{10.17}$$

with:

$$c_1(s, t) = G(s, t)\exp(-rR_D t) + r\int_0^t G(s, \tau)\,[R_D I_0(\zeta) + \sqrt{R_D\tau/(t-\tau)}\,I_1(\zeta)]$$
$$\exp[-r(R_D\tau + t - \tau)]\,d\tau \tag{10.18}$$

$$G(s, t) = \frac{1}{2}\operatorname{erfc}\sqrt{\frac{s(1-t)^2}{4t}} + \sqrt{\left(\frac{st}{\pi}\right)}\exp\left\{\frac{-s(1-t)^2}{4t}\right\}$$
$$-\frac{1}{2}(1 + s + st)e^s \operatorname{erfc}\sqrt{\frac{s(1+t)^2}{4t}} \tag{10.19}$$

$$\zeta = 2r\sqrt{R_D\tau(t-\tau)}; \qquad R_D = \frac{\rho_b k}{\theta}; \qquad r = \frac{k_r x}{v} \tag{10.20}$$

$$s = \frac{vx}{D}; \qquad t = \frac{vt}{x}; \qquad t_0 = \frac{vt_0}{x} \tag{10.21}$$

where I_0 and I_1 are modified Bessel functions of the first kind and of order 0 and 1, respectively. To maximize generality, the solution is expressed in four dimensionless variables. The variable R_D is a system constant since it is completely defined by properties of the chemical and medium. The variable r defines to what degree local equilibrium between solution concentration and adsorbed concentration is reached during the transfer process, and is essentially the same as the scaled variable $\hat{x}$, introduced in section 9.6 of the previous chapter. The *scaled* variables s and t reduce to the often used Péclet number, Pé (= vL/D), and the number of pore volumes, T ((10.12)), when effluent concentrations from a finite soil column are considered.

It should be mentioned here that all solutions given in this chapter are derived for a semi-infinite medium. When these solutions are used to calculate effluent concentrations by setting $x = L$, some small errors may be introduced. However, owing to the uncertainty of the exact physical processes at the exit of the column as well as the relatively small influence of the mathematical boundary conditions generally imposed on the system, i.e. the condition $\partial c/\partial x = 0$ at $x = L$ (see for example the discussions by Wehner and Wilhelm, 1956; Pearson, 1959; Van Genuchten and Wierenga, 1974), the solutions obtained for a semi-infinite medium should provide close approximations for those of a finite medium.

The analytical solution given above will now be used to investigate whether or not the kinetic model represents an improvement over the equilibrium model in describing the experimental data of Fig. 10.6. To be able to use this solution, the observed hysteresis effects have to be ignored. This presents no objection, however, since interest for the moment is only in the description of the break-through side of the effluent curve (hysteresis has no effect on this part of the curve as was shown in Figs. 10.4 and 10.6). It is further necessary to linearize the slightly non-linear adsorption isotherm of Fig. 10.7. The following procedure was used by Van Genuchten et al. (1977) to obtain this linearization. Denoting the linearized isotherm by ${}^{w}q = k_a^l c$, and requiring that the areas under the isotherm over the range 0—10 ppm (the column was leached with a 10-ppm 2,4,5-T solution) for both the linearized and the non-linear Freundlich equations be the same, one has from Fig. 10.7:

$$\int_0^{10} k_a^l c\,dc = \int_0^{10} 0.616\, c^{0.792}\,dc \qquad (10.22)$$

from which a value of 0.426 for the linearized adsorption constant, k_a^l, may be calculated.

Figure 10.8 compares the experimental data of Fig. 10.6 with curves based on (10.17)—(10.21), using values of the dimensionless rate coefficient, r, ranging from 0 to ∞. The curve labeled $r = 0$ represents the solution when no adsorption takes place (no exchange of material), while the curve for which $r \to \infty$ represents the limiting case of equilibrium adsorption. It is evident from Fig. 10.8 that no one value of r results in an acceptable description of the experimental data. It was found that the predictions could not be improved by either varying the Peclet number (Pé), or by including the non-linearity of the adsorption isotherm into a numerical solution of the same kinetic model. Similar plots were prepared, based on either model 2.4 or 2.5 (Table 10.1) and these showed only minor differences from those given in Fig. 10.8. Hence the kinetic model seems unable to fit the experimental data of Fig. 10.6.

Several other authors have compared predictions based on kinetic models with experimental data. Hornsby and Davidson (1973) compared the same kinetic model as discussed above with experimental data on the movement of Fluometuron through Norge loam. Concentration distributions versus

depth were presented for two pore-water velocities (v): 0.59 and 5.50 cm/h. The values of the ratio k_r/v for these two experiments were 5.93 and 0.64, respectively. By comparison, the ratio k_r/v for the curve labeled 7.0 in Fig. 10.8 equals 7.0/30, or 0.23 cm^{-1}. The rather high values of k_r/v used by Hornsby and Davidson (1973) suggest that their calculated curves would be the same or very close to those obtained with equilibrium solutions. The kinetic model used by these authors was not compared with the equilibrium model; hence no conclusions could be drawn on whether the kinetic model actually improved the description of the data or not.

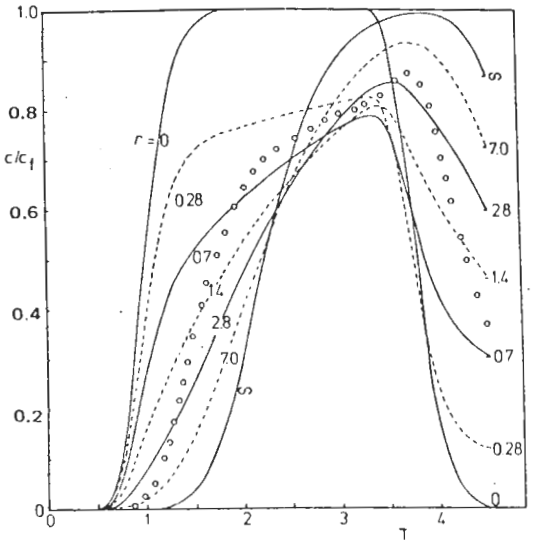

Fig. 10.8. Effect of the dimensionless rate coefficient, r, on calculated effluent curves for 2,4,5-T movement through Glendale clay loam. The open circles represent observed data points, and are the same as those shown in Fig. 10.6.

Van Genuchten et al. (1974) compared observed and calculated effluent concentrations for the movement of picloram through Norge loam. The calculated curves were based on both the equilibrium model and kinetic models 2.3 and 2.4 (Table 10.1). No satisfactory description of the experimental data could be obtained with any of the three models, except for a few experiments where the experimental data approached the equilibrium model. In that case the predictions of the kinetic and equilibrium models were about the same, since again rather high rate coefficients had to be used. The two kinetic models hence did not substantially improve the predictions of the data. The authors suggested that physical rather than kinetic phenomena produced the observed deviations between experiment and calculations.

Further experimental and calculated concentration profiles in soil columns

were presented by Huggenberger et al. (1972) for the movement of lindane through different soils. These authors used the model derived by Oddson et al. (1970), i.e. similar to (10.17) but with negligible dispersion. The solution of Oddson et al. (1970) is rather conveniently expressed with Goldstein's (1953) J-function, as follows:

$$\frac{c}{c_f} = \begin{cases} c_1(t) & 0 < t \leqslant t_0 \\ c_1(t) - c_1(t - t_0) & t > t_0 \end{cases} \tag{10.23}$$

where

$$c_1(t) = J(u, w) = \begin{cases} 0 & t \leqslant 1 \\ 1 - e^{-w} \int_0^u e^{-\tau} I_0(2\sqrt{w\tau}) d\tau & t > 1 \end{cases} \tag{10.24}$$

and

$$u = rR_D; \quad w = r(t - 1) \tag{10.25}$$

The use of this model by Huggenberger et al. (1972) resulted in a rather poor prediction of the experimental data. The chemical not only traveled much faster into the column than predicted by their model (the ratios k_r/v used by these authors ranged from 0.1 to 1.0 cm^{-1}), but the concentration distribution also appeared much more dispersed in the column than could be described by the no-dispersion model.

From the discussions above it appears that as yet no conclusive evidence exists that kinetic rate models are able to describe the often observed faster movement of the chemical than that predicted by equilibrium models. Obviously, more experimental evidence should be produced before definitive conclusions can be reached. However, the limited amount of experimental and theoretical investigations to date suggest that other, maybe more important, physical soil phenomena may have to be theoretically included if one is to describe satisfactorily the observed experimental data.

10.3.2. Physical non-equilibrium

Nearly all attempts to describe solute movement in soils have been based thus far on the convective–dispersive equation, appropriately modified to include such processes as adsorption and decay ((10.2)). Without adsorption and decay, this equation becomes:

$$\frac{\partial c}{\partial t} = D \frac{\partial^2 c}{\partial x^2} - v \frac{\partial c}{\partial x} \tag{10.26}$$

The general features of (10.26) have been discussed at length in section 9.5 ((9.51)). Except for small values of the dimensionless group vx/D, solute

distributions based on (10.26), whether plotted versus depth or as effluent curves, appear either sigmoidal in shape or more or less symmetrical (depending on the boundary conditions imposed at the soil surface).

As early as in 1961, Nielsen and Biggar (1961) observed serious deviations between the sigmoid-type break-through curves predicted with (10.26) and experimental curves for the movement of chloride through Oakley sand and glass beads. The lower the water content during their experiments, the more serious these deviations became. The solute appeared earlier in the effluent than could be predicted with the equation, while considerably more water was needed to reach a relative concentration of one. The early break-through of the chemical and the tailing towards complete displacement was attributed to the unsaturated conditions during their experiments. The authors argued that, when the water content decreases, more and more of the larger pores are eliminated for transport, resulting in a larger proportion of the water being located in relatively slow moving or immobile (stagnant or dead) zones. They suggested further that these almost stagnant or immobile water zones would act as sinks to ionic diffusion during the displacement process, leading to a nearly incomplete displacement. The occurrence of this stagnant water has been the subject of many other studies (Turner, 1958; Aris, 1959; Coats and Smith, 1964; Villermaux and Van Swaay, 1969; Gupta et al., 1973).

Several other conditions seem to influence the occurrence of immobile water, such as the presence of aggregates (Biggar and Nielsen, 1962; Green et al., 1972), or the use of undisturbed soil cores (McMahon and Thomas, 1974). The magnitude of the flow rate has also been linked with the presence of immobile water (Biggar and Nielsen, 1962; Gaudet et al., 1977).

Several theoretical studies have dealt with the presence of immobile liquid zones (see also chapter 9). Deans (1963) modified (10.26) to include the transfer by diffusion from mobile to immobile zones. His model was later used by Coats and Smith (1964), Villermaux and Van Swaay (1969), and Bennet and Goodridge (1970), and may be written in the following form:

$$\theta_m \frac{\partial c_m}{\partial t} + \theta_a \frac{\partial c_a}{\partial t} = \theta_m D \frac{\partial^2 c_m}{\partial x^2} - v_m \theta_m \frac{\partial c_m}{\partial x} \tag{10.27}$$

$$\theta_a \frac{\partial c_a}{\partial t} = k_a (c_m - c_a) \tag{10.28}$$

where the subscripts m and a refer to mobile and immobile liquid regions, respectively, and v_m is the average interstitial velocity of the liquid in the mobile region of the soil ($v_m = J^v/\theta_m$). The mass transfer coefficient k_a (day^{-1}) determines the rate of exchange between the two liquid regions. The model assumes that this rate of exchange is proportional to the concentration difference between the two liquid regions.

Equations (10.27) and (10.28) assume that no adsorption is present.

Van Genuchten and Wierenga (1976b) modified the model to include adsorption. The following set of differential equations resulted:

$$\theta_m \frac{\partial c_m}{\partial t} + \rho_b p \frac{\partial {}^w q_m}{\partial t} + \theta_a \frac{\partial c_a}{\partial t} + \rho_b (1-p) \frac{\partial {}^w q_a}{\partial t} = \theta_m D \frac{\partial^2 c_m}{\partial x^2} - v_m \theta_m \frac{\partial c_m}{\partial x} \tag{10.29}$$

$$\rho_b (1-p) \frac{\partial {}^w q_a}{\partial t} + \theta_a \frac{\partial c_a}{\partial t} = k_a (c_m - c_a) \tag{10.30}$$

where ${}^w q_m$ and ${}^w q_a$ represent the amounts adsorbed in the "mobile" and stagnant regions, respectively, both specified per unit mass of soil assigned to these two regions. The mass fraction of solid phase assigned to the mobile region on the basis of the corresponding adsorption capacity, Q, is indicated with the parameter p, such that ${}^w Q_m = p\,{}^w Q$, and ${}^w Q_a = (1-p)\,{}^w Q$. Equations (10.29) and (10.30) were derived by assuming that adsorption around the larger liquid-filled pores would not necessarily be the same as the adsorption around the micropores in the immobile zone. When a chemical moves through an aggregated and/or unsaturated soil, only part of the adsorption sites may be readily accessible for the invading solution. These sites are located around the larger pores and in direct contact with the mobile liquid. However, when an immobile liquid zone is present, some of the material can only be adsorbed by the stagnant part of the medium after it has diffused into the immobile zone, made up of dead (blind) pores and micropores inside aggregates. The division of the adsorption sites into two fractions, one fraction located in the 'mobile' region and one fraction in the stagnant region of the soil is characterized by the parameter p. When $p = 0$, all adsorption occurs away from the mobile liquid inside the stagnant region of the medium. In that case the model reduces to the one elaborated upon in section 9.6.

When it is assumed that equilibrium adsorption occurs, and the Freundlich isotherm is again used to describe the relation between sorbed and solution concentrations ((10.3)), the number of dependent variables may be decreased from four to two. Substitution of (10.3) into (10.29) and (10.30) leads then to:

$$[\theta_m + \rho_b p k n c_m^{n-1}] \frac{\partial c_m}{\partial t} + [\theta_a + \rho_b (1-p) k n c_a^{n-1}] \frac{\partial c_a}{\partial t} = \theta_m D \frac{\partial^2 c_m}{\partial x^2} - v_m \theta_m \frac{\partial c_m}{\partial x} \tag{10.31}$$

$$[\theta_a + \rho_b (1-p) k n c_a^{n-1}] \frac{\partial c_a}{\partial t} = k_a (c_m - c_a) \tag{10.32}$$

Several analytical solutions of (10.31) and (10.32) are available, provided, again, that the adsorption isotherm is linear ($n = 1$) and that no hysteresis between adsorption and desorption is present (Appendix B of Van Genuchten, 1974). For initial and boundary conditions equivalent to (10.2a) (c has to be replaced by c_m), the dimensionless solution is:

$$\frac{c_m}{c_f} = \begin{cases} c_1(s,t) & 0 < t \leqslant t_0 \\ c_1(s,t) - c_1(s,t-t_0) & t > t_0 \end{cases} \tag{10.33}$$

$$\frac{c_a}{c_f} = \begin{cases} c_2(s,t) & 0 < t \leqslant t_0 \\ c_2(s,t) - c_2(s,t-t_0) & t > t_0 \end{cases} \tag{10.34}$$

with:

$$c_1(s,t) = G(s,t)\exp(-rt/zR_f) + \frac{r}{R_f}\int_0^t G(s,\tau)\,H_1(t,\tau)\,d\tau \tag{10.35}$$

$$c_2(s,t) = r\int_0^t G(s,\tau)\,H_2(t,\tau)\,d\tau \tag{10.36}$$

$$G(s,t) = \frac{1}{2}\operatorname{erfc}\left\{\frac{s^{1/2}(zR_f - t)}{(4zR_f t)^{1/2}}\right\} + \left(\frac{st}{\pi z R_f}\right)^{1/2}\exp\left\{\frac{-s(zR_f - t)^2}{4zR_f t}\right\}$$
$$-\frac{1}{2}\left(1 + s + \frac{st}{zR_f}\right)e^s \operatorname{erfc}\left\{\frac{s^{1/2}(zR_f + t)}{(4zR_f t)^{1/2}}\right\} \tag{10.37}$$

$$H_1(t,\tau) = e^{-u-w}\left\{I_0(y)/z + I_1(y)/(1-z)\left(\frac{u}{w}\right)^{1/2}\right\} \tag{10.38}$$

$$H_2(t,\tau) = e^{-u-w}\left\{I_0(y)/(1-z) + I_1(y)/z\left(\frac{w}{u}\right)^{1/2}\right\} \tag{10.39}$$

$$y = 2\sqrt{uw}; \qquad u = \frac{r\tau}{zR_f}; \qquad w = \frac{r(t-\tau)}{(1-z)R_f} \tag{10.40}$$

The (italic) dimensionless variables are defined as:

$$z = \frac{\theta_m R_{f,m}}{\theta R_f}; \qquad s = \frac{v_m}{D}; \qquad t = \frac{vt}{x}; \qquad r = \frac{k_a x}{\theta v} \tag{10.41}$$

where:

$$\theta_m R_{f,m} = \theta_m + \rho_b p k; \quad \theta R_f = \theta + \rho_b k; \quad v = \frac{v_m \theta_m}{\theta} = \frac{J^v}{\theta} \tag{10.42}$$

Note that when effluent concentration distributions are considered (x = L), s and t, respectively reduce to the column Peclet number Pé (= $v_m L/D$) and the number of pore volumes leached through the column, T(= vt/L). In that case the solutions are expressed in four independent parameters, R_f, Pé, z, and r. Of these four parameters, the retardation factor is the most easily determined independently, for example, from batch equilibration studies. The remaining three parameters however are less easy to quantify. The parameter z, for example, depends on the fraction of mobile liquid in the medium $\phi_m (= \theta_m/\theta)$ and the fraction of the sorption sites located in the dynamic region of the soil (p). These quantities are difficult to quantify a priori. Generally elaborate curve-fitting techniques have to be used to determine their values (Van Genuchten and Wierenga, 1977).

Referring to (9.48) and (9.102) of the previous chapter it is pointed out that for $p = 0$ (all adsorption sites assumed to be located within the stagnant region) one obtains $z = \theta_m/(\theta + \rho_b k)$, such that $(1 - z) = A\phi_a$.

Before continuing the discussion of the 2,4,5-T effluent data given in the previous two sections, a sensitivity analysis will be carried out for each of the four dimensionless parameters z, R_f, Pé, and r. Each variable was allowed to vary while keeping the remaining three constant. Results are shown in Figs. 10.9—10.12. The concentration curves were plotted versus pore volumes, assuming that the chemical was in the feed solution during the first three pore volumes.

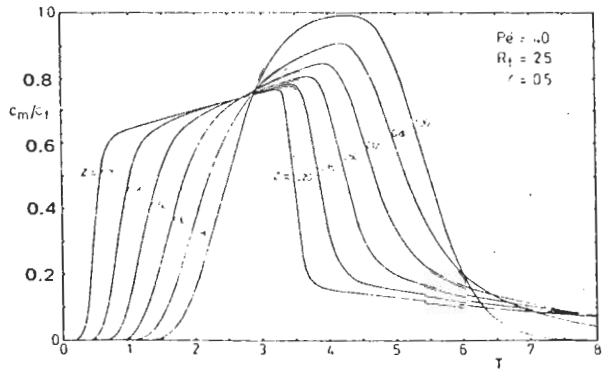

Fig. 10.9. Effect of the dimensionless variable z on calculated effluent curves from an aggregated sorbing medium.

The influence of the parameter z is shown in Fig. 10.9. This parameter defines the relative contribution of the mobile phase to the overall retardation of a solute front in the system. In the limiting case when $z = 1$, no immobile water is present ($\phi_m = 1$) and all sorption sites are immediately accessible for the displacing chemical solution ($p = 1$). The model then reduces to the convective—dispersive equation, modified for linear adsorption ((9.45)), and the effluent curve becomes nearly symmetrical in shape

(Fig. 10.9). When a large immobile liquid zone is present ($\theta_m \ll \theta$), the velocity of the liquid in the mobile region will increase because the convective transfer processes are confined to a smaller cross-sectional area ($v_m = J^v/\theta_m$). Particularly the combination of $\phi_m \ll 1$ and $p \ll 1$ (stagnant regions containing a substantial fraction of the sorption sites) leads to an early break-through of the chemical (a "faster" moving liquid with relatively less retardation in the mobile region). At the same time the chemical may diffuse slowly from the mobile into the stagnant region, where part of it will be adsorbed. This diffusion process will continuously remove material from the mobile region, resulting in a "tailing" phenomenon as manifested by the slow increase in concentration after the first appearance of the chemical in the effluent (Fig. 10.9). The extreme case when $z = 0.4$ may occur when the medium is highly aggregated or exhibits severe channeling (also for certain fractured media). In that case the effluent curves become very distorted (asymmetrical). It should be noted that the analytical solution ((10.33)–10.42)) breaks down when $\theta_m = \theta$ and $p < 1$ (some sorption sites are located in "dry" stagnant regions, possibly in densely compacted aggregates or between closely packed soil particles). Some of the sites are then assumed to be completely inaccessible for the displacing fluid. Total adsorption as seen by the "undisturbed" soil will now become less than that inferred from static (batch) equilibrium measurements on 'disturbed' soil ($R_{f,m} < R_f$). The solute distribution in this case will retain its nearly symmetrical shape as predicted by the linear equilibrium model (section 10.2.1), but the resulting effluent curve will be displaced to the left of the curve labeled 1.0 in Fig. 10.9. This particular approach was used by Van Genuchten et al. (1974) and Wood and Davidson (1975) to model the relatively faster movement of the chemical through the soil.

The influence of the retardation factor is shown in Fig. 10.10. As expected, the chemical appears later in the effluent when R_f increases (i.e. when sorption increases). Also the peak concentration seems to decrease

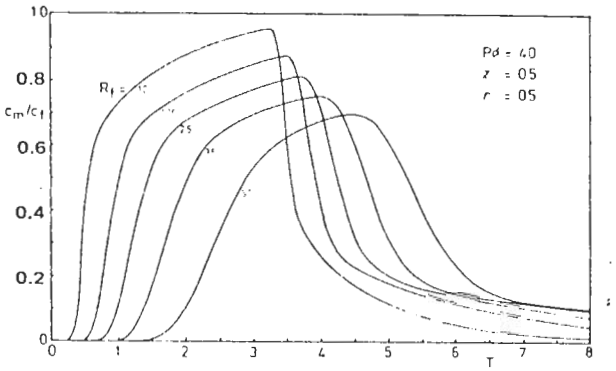

Fig. 10.10. Effect of the retardation factor, R_f, on calculated effluent curves from an aggregated sorbing medium.

somewhat with increasing adsorption. When $R_f = 1$, no adsorption occurs and the model simulates the movement of an inert chemical through an aggregated medium. Tailing in this case becomes less pronounced (Fig. 10.10), because no adsorption can take place in the stagnant region and the chemical can be stored only in the immobile liquid of the stagnant region. Hence relatively less chemical has to diffuse into the immobile zone.

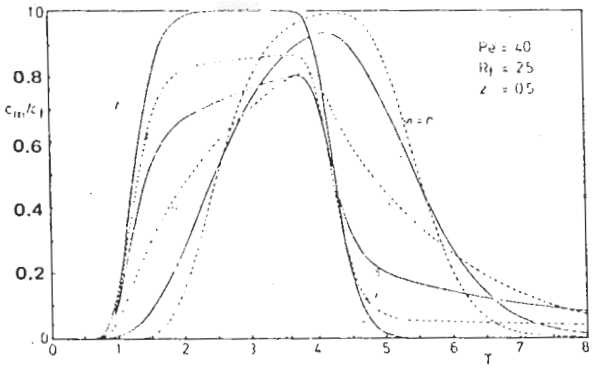

Fig. 10.11. Effect of the dimensionless mass transfer coefficient, r, on calculated effluent curves from an aggregated sorbing medium.

Fig. 10.11 shows the effect of the mass transfer coefficient r on the shape and position of the effluent concentration distributions. When $r = 0$ no material can diffuse into the stagnant region of the soil, and adsorption is confined to the dynamic region of the soil. In this case, the effluent curve again acquires a nearly symmetrical shape. When r is small, the exchange by diffusion between dynamic and stagnant regions is still very slow, resulting in the bulk of the chemical traveling through the medium nearly unaffected by the exchange. However, the stagnant zone keeps exchanging material with the mobile liquid, resulting in extensive tailing, both during break-through and elution. With increasing values of the mass transfer coefficient, the rate of exchange increases, eventually leading to a new equilibrium where the concentrations in mobile and immobile liquid are identical ($c_m = c_a$). This limiting case is represented by the curve $r \to \infty$. The curves given in Fig. 10.11 are nearly identical to those shown in Fig. 10.8. This is not surprising because the intra-aggregate diffusion model ((10.31) and (10.32)) is mathematically similar to the kinetic adsorption model ((10.2) and (10.16)).

Finally, the influence of the column Peclet number, Pé, is shown in Fig. 10.12. The influence of Pé on the shape of the calculated curves is relatively small. Note the discontinuities of the curve for which Pé = ∞, at both 1.3, and 4.3 pore volumes. From Fig. 10.12 one may conclude that an approximate value of the dispersion coefficient generally is sufficient when describing the leaching of chemical through aggregated, unsaturated soils. An interesting observation may be made when comparing Figs. 10.11 and 10.12. When r is large, a small change in the value of this coefficient seems to have

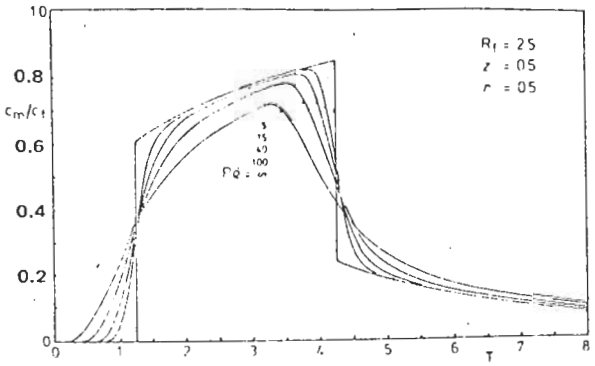

Fig. 10.12. Effect of the Peclet number, Pé, on calculated effluent curves from an aggregated sorbing medium.

the same effect as a change in the dispersion coefficient. Also, from Fig. 10.8, when the kinetic rate coefficient is large, i.e. near equilibrium adsorption, a small change in this coefficient results in effects which could also be obtained in an approximate way by a change in the dispersion coefficient (see the relevant discussion of Fig. 9.17). These are rather important observations. It seems highly probable that when the dispersion coefficient is fitted to experimentally obtained concentration profiles, it will also include any small kinetic or intra-aggregate diffusion effects which may be present.

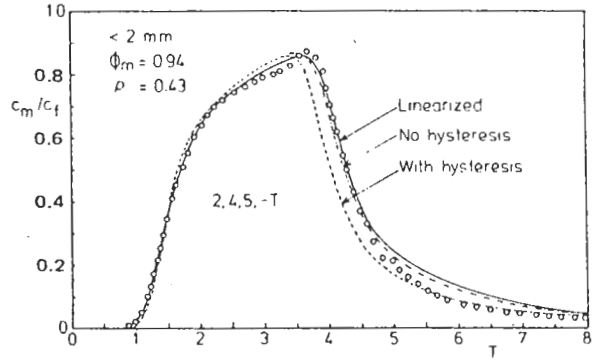

Fig. 10.13. Calculated and observed effluent curves for 2,4,5-T movement through Glendale clay loam. The open circles represent observed data points, and are the same as those shown in Fig. 10.6.

The question remains whether the intra-aggregate diffusion model is able to better describe the previously shown experimental 2,4,5-T effluent data than was possible with either the equilibrium model (Fig. 10.6) or the kinetic model (Fig. 10.8). Figure 10.13 shows a best-fit comparison of the experimental data with the diffusion model, using a value of 0.426 for the

linearized adsorption constant k_a^l. Values of the three curve-fitted parameters, z, Pé, and r, are shown in the Figure. An important improvement in the description of the data is obtained; especially the front side of the effluent curve is well described by the model. The same Figure also shows the effects of hysteresis and non-linear adsorption on the calculated results. It appears that these influences are rather small. The slope of the break-through side of the curve increases slightly when non-linear adsorption is considered (section 10.2.1). The inclusion of hysteresis in the model again does not affect the front part of the curve, but it results in an earlier decrease in concentration during elution of the chemical, as well as more prolonged tailing at the higher pore volumes. However, from Fig. 10.13 it is clear that hysteresis does not affect the results to any great extent. Such a conclusion is not possible when intra-aggregate diffusion is neglected, as was shown in Figs. 10.4 and 10.6. Thus for the conditions of this study, intra-aggregate exchange of 2,4,5-T between dynamic and stagnant regions seems to be far more important than the observed hysteresis in the adsorption–desorption process.

The curves representing non-linear adsorption, with and without hysteresis (Fig. 10.13), were obtained with a numerical solution of (10.31) and (10.32) (Van Genuchten and Wierenga, 1976a). To be able to use this solution, one needs separate estimates of the parameters p and θ_m. These may be obtained by leaching the same column with an inert material such as tritium. Figure 10.14a shows effluent distributions of tritiated water which were obtained from the same column for which the 2,4,5-T data were obtained. The effluent data of tritium were also fitted to the linearized intra-aggregate diffusion model, resulting in the parameter values shown in the Figure. A small retardation of the tritium was observed during its displacement through the column. The linearized adsorption constant k_a^l in the Freundlich isotherm was found to be 0.009, equivalent to a retardation factor R_f of 1.027. Estimates of the parameters p and $\phi_m (= \theta_m/\theta)$ may then be obtained by assuming that they are the same for both tritium and 2,4,5-T movement. From the definitions of z ((10.41)), $R_{f,m}$, and R_f, one obtains:

$$zR_f = \phi_m + p(R_f - 1) \tag{10.43}$$

Using the values for 2,4,5-T (Fig. 10.13; $R_f = 2.225$; $z = 0.661$) and tritiated water (Fig. 10.14a; $R_f = 1.027$; $z = 0.926$), (10.43) leads then to:

$$\begin{aligned} (0.661)(2.225) &= \phi_m + p(1.225) \qquad (2,4,5\text{-T}) \\ (0.926)(1.027) &= \phi_m + p(0.027) \qquad (^3H_2O) \end{aligned} \tag{10.44}$$

or:

$$\begin{aligned} \phi_m &= \frac{\theta_m}{\theta} = 0.94 \\ p &= 0.43 \end{aligned} \tag{10.45}$$

The above derivation assumes that the ratio of mobile to total water (θ_m/θ) for the two experiments is the same. This assumption seems reasonable since the two displacements were carried out at approximately the same flow velocities (J^V equals 5.11 and 5.09 cm/day, respectively for 2,4,5-T and tritium) and at the same water contents (θ equaled 0.473 and 0.460, respectively). The assumption that p is also the same for the two chemicals, however, may not be entirely true owing to the different adsorption mechanisms for 2,4,5-T and tritium. The herbicide 2,4,5-T is adsorbed by the organic matter fraction of the soil (O'Connor and Anderson, 1974), while the observed tritium retardation may be caused by some isotopic exchange of tritium with crystal-lattice hydroxyls of the clay fraction of the soil, or by replacement of some exchangeable cations by $^3H^+$. However, by changing the value of p for tritium slightly and considering the small value of the retardation factor for tritium, it is easily demonstrated that the values of ϕ_m and p (for 2,4,5-T) will remain essentially the same.

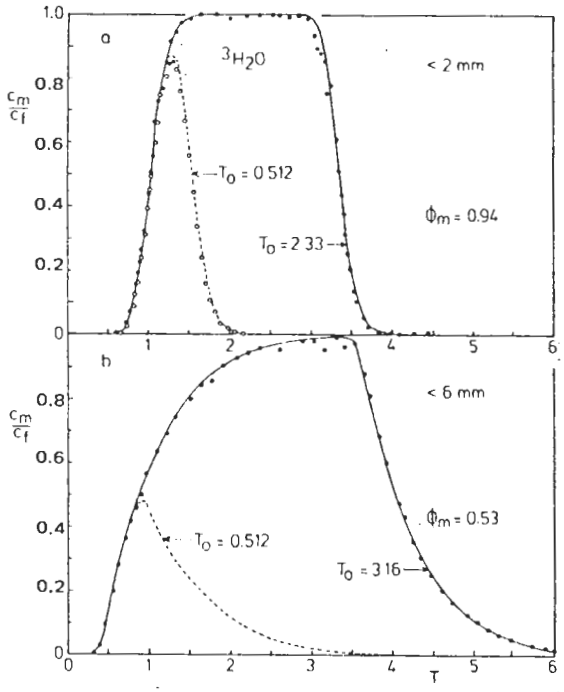

Fig. 10.14. Calculated and observed effluent curves for tritium movement through Glendale clay loam. Results were obtained with two different aggregate sizes and bulk densities, but with approximately the same pore-water velocities. a: < 2 mm aggregates, $\rho_b = 1.36$ g/cm^3, $J^V = 5.09$ cm/day, $\theta = 0.460$ cm^3/cm^3, $z = 0.926$, Pé $= 95$, $r = 1.47$ and $R_f = 1.027$. b: < 6 mm aggregates, $\rho_b = 1.13$, $J^V = 5.54$ cm/day, $\theta = 0.399$ cm^3/cm^3, $z = 0.531$, Pé $= 35$, $r = 1.54$, and $R_f = 1.025$.

The value of the parameter ϕ_m as derived above indicates that about 94% of the water in the column may be considered mobile water, and that only 6% is immobile. This small amount of immobile water has little effect on the calculated results for tritium (Fig. 10.14a). In fact, the effluent distribution of this example could be described equally well with appropriate solutions of the convective–dispersive equation (10.26). When the amount of immobile water increases, however, such a description becomes exceedingly difficult. Figure 10.14b represents a more extreme case where nearly 50% of the water in the column is immobile. Note that the effluent curves, for both a short and long solute pulse, become much more asymmetrical than the approximately symmetrical ones shown in Fig. 10.14a. The curves in Fig. 10.14b were obtained using larger aggregates in the soil column, as well as a lower bulk density. Both conditions seem to favor the presence of stagnant liquid regions in the soil. When larger aggregates are present, the pore-size distribution is likely to become much broader owing to the creation of larger interaggregate pores and the existence of a significant amount of small intra-aggregate (micro) pores. An increase in aggregate size also increases the diffusion length between mobile and immobile regions, leading to a slower exchange of material between the two liquid regions. The bulk density may also affect the amount of immobile water present. When the bulk density decreases, the pore-size distribution is also likely to become broader, owing to the creation of larger interaggregate pores (given the same aggregate size). The broader the pore-size distribution, the broader also the pore-water velocity distribution will become: some water will move faster in the soil, and some water will not move at all or only very slowly compared to the average pore-water velocity. Hence, the diffusion processes between fast and slowly moving liquid zones become more important. The curves shown in Fig. 10.14b may be typical for the leaching processes in undisturbed aggregated field soils.

The influence of aggregate size on the effluent distributions for 2,4,5-T seems to be less than for tritium. Figure 10.15 shows the effluent concentration profiles obtained from aggregates of less than 6 mm (experiment 4-1 of Van Genuchten et al., 1977). The chemical appears slightly earlier in the effluent compared to the experimental data shown in Fig. 10.13, but this is primarily a result of the presence of more immobile liquid. The value of p found for the larger aggregates is only slightly smaller than for the smaller (< 2 mm) aggregates: 0.40 vs. 0.43. This value was not significantly affected by either aggregate size or bulk density (Van Genuchten et al., 1977). The average value determined was 0.40, indicating that 40% of the sorption sites are located around the larger, liquid-filled pores of the dynamic region, while 60% of the sites are located either inside aggregates or along blind (dead-end) pores.

Figure 10.16 further shows the effluent concentration distributions of boron (H_3BO_4) obtained from 30-cm long columns packed with the same

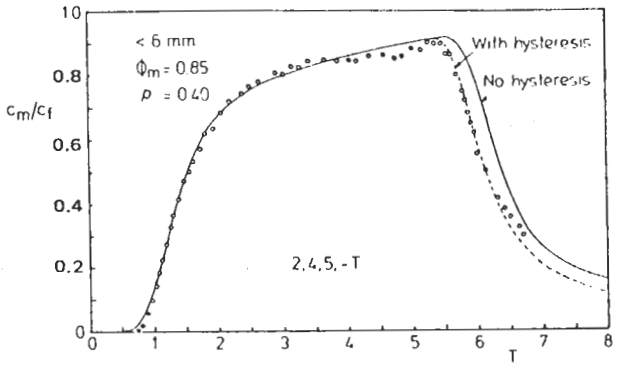

Fig. 10.15. Calculated and observed effluent curves for 2,4,5-T movement through Glendale clay loam. The following soil-physical data were used in the calculations: $\rho_b = 1.31$ g/cm^3, $J^V = 16.81$ cm/day, $\theta = 0.456$ cm^3/cm^3, $t_0 = 4.028$ days and $L = 30$ cm.

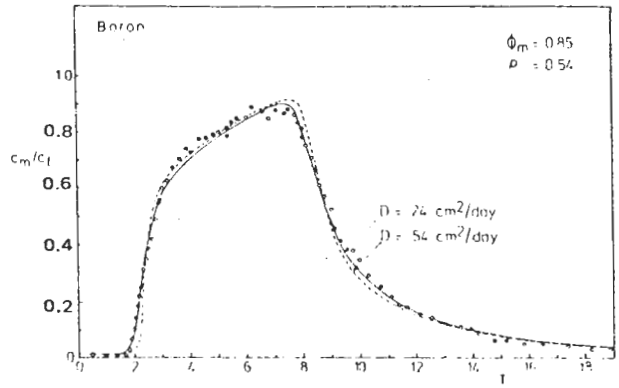

Fig. 10.16. Calculated and observed effluent curves for boron movement through Glendale clay loam. The following soil-physical data were used in the calculations: $\rho_b = 1.22$ g/cm^3, $J^V = 17.12$ cm/day, $\theta = 0.445$ cm^3/cm^3, $t_0 = 5.06$ days and $L = 30$ cm.

(6-mm aggregate-sized) Glendale clay loam soil material. The equilibrium adsorption isotherm for this chemical and soil was adequately described with the non-linear isotherm $^{w}q = 2.77\ C^{0.672}$ (Van Genuchten, 1974). No hysteresis was observed for this chemical. In a separate experiment with tritium, the fraction of mobile liquid, ϕ_m, was found to be 0.85, and the Peclet number, Pé, was found to be 56. The dashed line in Fig. 10.16 is based on these parameter values. Although the description of the experimental data is reasonable, it may be improved by increasing the value of the dispersion coefficient (solid line). Boron adsorption during batch equilibration was found to be complete only after shaking the chemical and soil for about 1—5 h. Hence, some kinetic effects are likely to be present during boron movement at a volumetric flux, J^V, of 17.12 cm/day. It was shown

earlier (Fig. 10.8) that the kinetic adsorption mechanism will smear the concentration front in a way which is very much similar to an increase in dispersive transport (Fig. 10.12). Because the present study assumes equilibrium adsorption, the observed small kinetic effects may be included in the model by increasing the dispersion coefficient.

The fraction of the sorption sites located in the dynamic region of the soil (p) for the boron experiment is higher than the value found for 2,4,5-T (0.54 vs. 0.40). This indicates that relatively more boron is adsorbed in the vicinity of the main flowing paths of the moving liquid. Apparently more boron is adsorbed at the exterior of the aggregates, while relatively more 2,4,5-T is adsorbed inside the aggregates. The differences in p for boron and 2,4,5-T are probably indicative of the different adsorption mechanisms for the two chemicals. Boron adsorption presumably takes place on the mineral fraction of the soil (Rhoades et al., 1970), while 2,4,5-T adsorption occurs on the organic fraction.

10.3.3. Mobile and immobile concentration distributions in soils

The success of the intra-aggregate diffusion model in describing experimental data for the movement of tritium, 2,4,5-T, and boron suggests the importance of physical processes associated with the leaching of chemicals in the field. Many field soils exhibit some kind of aggregation or channeling; such conditions seem to favor the existence of large zones of immobile water. In addition, leaching processes in the field frequently occur under unsaturated conditions and often at relatively low flow rates, both of which also favor more immobile liquid. Wild (1972) studied the movement of water and mineralized nitrate (formed from soil organic matter) under a bare field site, and found that the leaching of the nitrate was much more gradual than could be predicted by miscible displacement theories. He suggested that water was moving mainly through the larger cracks and channels, and hence was unable to leach the nitrate that was contained largely in the relatively immobile regions of the aggregates (peds). Gumbs and Warkentin (1975) also concluded that water was moving through the largest interaggregate pores during infiltration into an aggregated clay soil under zero pressure. The wetting front apparently bypassed some of the aggregates, which then remained relatively dry for some period of time. These two examples suggest that the infiltrating water may not necessarily displace the moisture inside the aggregates, but may leave this immobile water relatively undisturbed during its movement through the soil. When the invading liquid contains a solute, displacement in the aggregates and away from the larger cracks and channels will become strongly dependent upon diffusion processes, and should be incomplete for a considerable amount of time after the water/solute front has passed.

Considerable evidence for the existence of immobile liquid zones in the

field may be found in a recent study by Quisenberry and Phillips (1976). Small pulses of water and chloride were applied to two field soils and the downward propagation of these pulses was followed in time. Both the water and solute moved rapidly, even though the moisture content during the experiments was generally less than the field capacity of the soil. The rapid migration of both water and solute beyond the lowest (90 cm) sampling depth suggests that it was the applied water which moved through the soil and not the initial soil water which could have been displaced by the feed solution. If the surface-applied water had displaced the initial soil water during its movement downwards, the chloride should have been measured near the soil surface (as was the case in studies reported by Warrick et al. (1971), and Kirda et al. (1973)). Apparently channeling, especially beneath the Ap horizon, was responsible for the rapid movement of both water and chloride, resulting in little or no convective displacement away from the channels. It seems evident that in this case a considerable amount of dead water is present in the soil, probably much higher than the 50% observed for the data in Fig. 10.14 (see also the recent study by Wild and Babiker, 1976).

When such large percentages of stagnant water are present, it is evident that the conventional convective–dispersive equation may be inadequate in describing the leaching process. The intra-aggregate diffusion model may prove to be a better model for such conditions. An important feature of this model is its ability to differentiate between such mobile and immobile liquid zones. Figure 10.17 gives an example of the type of distributions one may obtain with this model. The solute profiles inside a 30-cm long soil column were obtained with (10.33) and (10.34), using the same parameter values as were used for the calculated curve shown in Fig. 10.14b. It was assumed, however, that the solute was in the feed solution for only 1 day ($t_0 = 1$). Figure 10.17 shows that the concentration in the immobile liquid (c_a) is considerably different from that in the mobile liquid (c_m). Owing to the diffusion of the solute into and out of the immobile zone, the immobile concentration lags behind the mobile concentration. The weighted average concentration, $\langle c \rangle$, at any point in the column is given by:

$$\langle c \rangle = \phi_m c_m + (1 - \phi_m) c_a \tag{10.46}$$

Since the fraction of mobile water was 0.53 for this experiment it follows that the average concentration in the profile is approximately the average of c_m and c_a.

When a sorbing medium is considered, the differences between mobile and immobile concentrations become even more pronounced. Figure 10.18 shows the distributions of 2,4,5-T, inside a 30-cm long soil column, obtained with the same data as given in Fig. 10.15. Also in this case 60% of the adsorption occurs in stagnant regions, but because of the increased sorptive capacity of the soil much more material can diffuse into the stagnant region before adsorption in this part of the soil will be complete. As a result, the

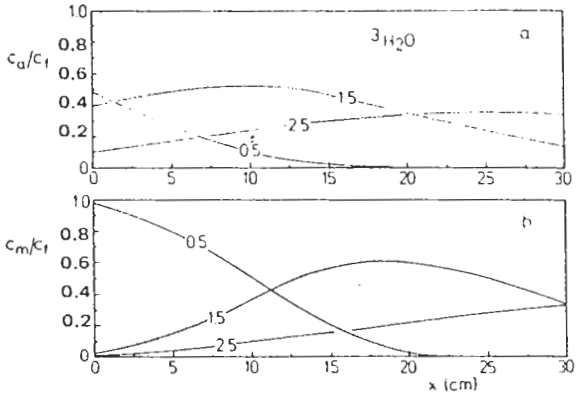

Fig. 10.17. Concentration profiles inside a 30 cm long soil column at different times during leaching with a short pulse (t_0 = 1 day) of tritiated water. Numbers on the curves indicate times (days) after leaching is initiated. Values of the parameters used to construct the curves are given in Fig. 10.14b.

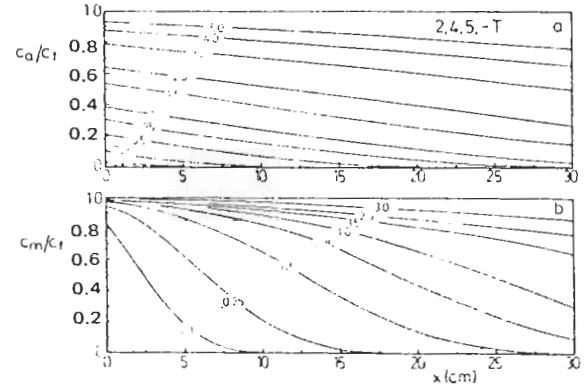

Fig. 10.18. Concentration profiles inside a 30 cm long soil column at different times during leaching with a continuous feed solution of 2,4,5-T. Numbers on the curves indicate times (days) after leaching is initiated. Values of the parameters used to construct the curves are given in Figure 10.15.

concentration in the immobile region will increase much more slowly than when tritium movement is considered. For example, at 20 cm from the soil surface, the relative concentration in the mobile phase reaches 0.5 after 0.8 day, while at this depth it takes about 2.4 days or three-times as long for the immobile liquid to reach a relative concentration of 0.5. That fraction of the chemical which diffuses into the stagnant region of the soil and which will remain in solution may be calculated by considering transport equation (10.32), which governs the exchange between mobile and stagnant regions of the soil. The first term on the left of (10.32) represents the material which

will be stored in the immobile liquid, while the second term gives the material which is actually adsorbed by the stagnant region. Assuming linear adsorption ($n = 1$), the fraction remaining in the solution is found to be equal to $\theta_a/\{\theta_a + (1 - p)\rho_b k\}$.

For the data given in Fig. 10.15, one may calculate that only 17% of the chemical which diffuses into the stagnant region of the soil will remain in solution, the remaining 83% being adsorbed by this part of the soil. For tritium, however, nearly 100% will remain in solution. Thus, when sorption increases, relatively more material can diffuse into the stagnant region. Since this diffusion process is very slow compared to the rate at which the bulk of the chemical moves through the soil, the differences between mobile and immobile concentrations are likely to increase when sorption further increases.

Solute distributions like those shown in Figs. 10.17 and 10.18 may also be helpful in understanding at least some of the factors controlling the variability of sampling results obtained when suction cups are used for solute measurements in the field (England, 1974; Hansen and Harris, 1975). A suction cup essentially represents a point source of suction in the soil matrix, and the suction applied through the cups to the soil will determine, in part, the minimum pore size that will be drained in the immediate vicinity of the cup. It is obvious that the physical make-up of the cup as well as the way they are installed, play important roles in the performance of the cups (Parizek and Lane, 1970). The microscopic location of the porous cup in the medium, however, seems to be of prime importance. When the cup is installed inside a large soil aggregate (or ped), or away from a channel or large interaggregate pore, it is likely that mainly immobile liquid will be withdrawn through the sampler device. This will also be the case when the cup, during its installment, is pressed into the soil too strongly, so that the soil becomes locally compacted. The immobile liquid which will be withdrawn from the soil in such cases, may have a concentration quite different from that of the mobile liquid, as evidenced by the distributions shown in Figs. 10.17 and 10.18.

One may also expect a concentration—time effect when soil water is withdrawn through suction cups. This effect will depend upon the history of the solute distribution. For example, when a suction cup is installed such that it is in contact with both macropores and micropores, the sampler is likely to first withdraw mainly mobile liquid. With increasing time, and depending upon the conductivity of the individual pores, the mobile liquid around the porous cup will drain slowly away, leading to a lower rate of water uptake by the sampler. When a sufficiently large pressure is applied, more and more liquid will subsequently be withdrawn from the immobile regions through the smaller micropores. When this is the case, the solute concentration sampled is likely to change with time. Referring to the distributions of Fig. 10.18, for example, one may always expect a decrease in

concentration with time, since the immobile concentration lags behind the mobile concentration. For the distributions given in Fig. 10.17, however, the concentration will decrease with increasing sampling length only when the mobile concentration is higher than the immobile concentration (e.g. in the upper 15^{cm} after 1 day). After 1.5 days this situation is reversed and the concentration of the liquid withdrawn through the cups is likely to increase during sampling in the upper part of the column.

Obviously any of several factors may account for the serious concentration variability sometimes observed in the field during suction cup cosampling. The intra-aggregate diffusion model results of this chapter, however, appear to provide a quantitative description and explanation for the important soil-physical phenomena which no doubt are a major contributor to this observed variability for many soils.

ACKNOWLEDGEMENTS

This work was supported, in part, by funds obtained from EPA Grant No. R803827-01, the Northeastern Forest Experiment Station of the USDA, Grant No. 23-586, and NSF Grant No. ENG-75-19184.

REFERENCES

Aris, R., 1959. Diffusion and reaction in flow systems of Turner's structures. Chem. Eng. Sci., 10: 80—87.

Bailey, G.W., White, J.L. and Rothberg, T., 1968. Adsorption of organic herbicides by montmorillonite. Role of pH and chemical character of adsorbate. Soil Sci. Soc. Am. Proc., 32: 222—234.

Ballaux, J.C. and Peaslee, D.E., 1975. Relationships between sorption and desorption of phosphorous by soils. Soil Sci. Soc. Am. Proc., 39: 275—278.

Bennet, A. and Goodridge, F., 1970. Hydrodynamic and mass transfer studies in packed adsorption columns: I. Axial liquid dispersion. Trans. Inst. Chem. Eng., 48: 232—240.

Biggar, J.W. and Nielsen, D.R., 1962. Miscible displacement: II. Behavior of tracers. Soil Sci. Soc. Am. Proc., 26: 125—128.

Cleary, R.W. and Adrian, D.D., 1973. Analytical solution of the convective—dispersive equation for cation adsorption in soils. Soil Sci. Soc. Am. Proc., 37: 197—199.

Coats, K.H. and Smith, B.D., 1964. Dead-end pore volume and dispersion in porous media. Soc. Pet. Eng. J., 4: 73—84.

Davidson, J.M. and Chang, R.K., 1972. Transport of picloram in relation to soil-physical conditions and pore-water velocity. Soil Sci. Soc. Am. Proc., 36: 257—261.

Deans, H.A., 1963. A mathematical model for dispersion in the direction of flow in porous media. Soc. Pet. Eng. J., 3: 49—52.

Enfield, C.G., Harlin, C.C. Jr., and Bledsoe, B.E., 1976. Comparison of five kinetic models for orthophosphate reactions in mineral soils. Soil Sci. Soc. Am. J., 40: 243—249.

England, C.B., 1974. Comments on "A technique using porous cups for water sampling

at any depth in the unsaturated zone", by Warren W. Wood. Water Resour. Res., 10: 1049.

Farmer, W.J. and Aochi, Y., 1974. Picloram sorption by soils. Soil Sci. Soc. Am. Proc., 38: 418—423.

Fava, A. and Eyring, H., 1956. Equilibrium and kinetics of detergent adsorption — A generalized equilibration theory. J. Phys. Chem., 65: 890—898.

Gaudet, J.P., Jégat, H., Vachaud, G. and Wierenga, P., 1977. Solute transfer, with exchange between mobile and stagnant water, through unsaturated sand. Soil Sci. Soc. Am. J., 41: 665—671.

Gershon, N.D. and Nir, A., 1969. Effects of boundary conditions of models on tracer distribution in flow through porous mediums. Water Resour. Res., 5: 830—839.

Goldstein, F.R.S., 1953. On the mathematics of exchange processes in fixed columns: I. Mathematical solutions and asymptotic expansions. Proc. R. Soc., Lond., 219: 151—185.

Green, R.E., Rao, P.S.C. and Corey, J.C., 1972. Solute transport in aggregated soils: tracer zone shape in relation to pore-velocity distribution and adsorption. Proc. 2nd Symp. Fundamentals of Transport Phenomena in Porous Media. Guelph, August 7—11, IAHR—ISSS, 2: 732—752.

Gumbs, F.A. and Warkentin, B.P., 1975. Prediction of infiltration of water into aggregated clay soil samples. Soil Sci. Soc. Am. Proc., 39: 255—263.

Gupta, R.K., Millington, R.J. and Klute, A., 1973. Hydrodynamic dispersion in unsaturated porous media. I. Concentration distribution during dispersion. J. Indian Soc. Soil Sci., 21: 1—7.

Gupta, S.P. and Greenkorn, R.A., 1976. Solution for radial-flow with non-linear adsorption. J. Environ. Eng. Div., Am. Soc. Cir. Eng., 102: 87—94.

Hansen, E.A. and Harris, A.R., 1975. Validity of soil-water samples collected with porous ceramic cups. Soil Sci. Soc. Am., Proc., 39: 528—536.

Hashimoto, I., Deshpande, K.B. and Thomas, H.C., 1964. Péclet numbers and retardation factors for ion exchange columns. Ind. Eng. Chem. Fund., 3: 213—218.

Hendricks, D.W., 1972. Sorption in flow through porous media. In: Fundamentals of Transport Phenomena in Porous Media. Developments in Soil Science, 2. Elsevier, Amsterdam, pp. 384—392.

Hornsby, A.G. and Davidson, J.M., 1973. Solution and adsorbed fluometuron concentration distribution in a water-saturated soil: experimental and predicted evaluation. Soil. Sci. Soc. Am. Proc., 37: 823—828.

Huggenberger, F., Letey, J. and Farmer, W.J., 1972. Observed and calculated distribution of lindane in soil columns as influenced by water movement. Soil Sci. Soc. Am. Proc., 36: 544—548.

IBM, 1967. System/360 Continuous System Modeling Program (360A-CX-16X), User's Manual. Data Processing Division, 122 East Post Road, White Plains, New York, N.Y.

Kay, B.D. and Elrick, D.E., 1967. Adsorption and movement of lindane in soils. Soil Sci., 104: 314—322.

Kirda, C., Nielsen, D.R. and Biggar, J.W., 1973. Simultaneous transport of chloride and water during infiltration. Soil Sci. Soc. Am. Proc., 37: 339—345.

Lai, Sung-Ho and Jurinak, J.J., 1971. Numerical approximation of cation exchange in miscible displacement through soil columns. Soil Sci. Soc. Am. Proc., 35: 894—899.

Lapidus, L. and Amundson, N.R., 1952. Mathematics of adsorption in beds: VI. The effect of longitudinal diffusion in ion exchange and chromatographic columns. J. Phys. Chem., 56: 984—988.

Leenheer, J.A. and Ahlrichs, J.L., 1971. A kinetic and equilibrium study of the adsorption of carbaryl and parathion upon soil organic matter surfaces. Soil Sci. Soc. Am., Proc., 35: 700—705.

Lindstrom, F.T., Haque, R., Freed, V.H. and Boersma, L., 1967. Theory on the movement of some herbicides in soils. Environ. Sci. Technol., 1: 561–565.

Lindstrom, F.T. and Boersma, L., 1970. Theory of chemical transport with simultaneous sorption in a water saturated porous medium. Soil Sci., 110: 1–9.

Lindstrom, F.T., Boersma, L. and Stockard, D., 1971. A theory on the mass transport of previously distributed chemicals in a water saturated sorbing porous medium. Isothermal cases. Soil Sci., 112: 291–300.

McMahon, M.A. and Thomas, G.W., 1974. Chloride and tritiated water flow in disturbed and undisturbed soil cores. Soil Sci. Soc. Am. Proc., 38: 727–732.

Nielsen, D.R. and Biggar, J.W., 1961. Miscible displacement in soils: I. Experimental information. Soil. Sci. Soc. Am. Proc., 25: 1–5.

O'Connor, G.A. and Anderson, J.U., 1974. Soil factors affecting the adsorption of 2,4,5-T. Soil Sci. Soc. Am. Proc., 38: 433–436.

Oddson, J.K., Letey, J. and Weeks, L.V., 1970. Predicted distribution of organic chemicals in solution and adsorbed as a function of position and time for various chemical and soil properties. Soil Sci. Soc. Am. Proc., 34: 412–417.

Parizek, R.R. and Lane, B.E., 1970. Soil-water sampling using pan and deep pressure–vacuum lysimeters. J. Hydrol., 11: 1–21.

Pearson, J.R.A., 1959. A note on the 'Danckwerts' boundary conditions for continuous flow reactors. Chem. Eng. Sci., 10: 281–284.

Quisenberry, V.L. and Phillips, R.E., 1976. Percolation of surface-applied water in the field. Soil Sci. Soc. Am., J., 40: 484–489.

Rhoades, J.D., Ingvalson, R.D. and Hatcher, J.T., 1970. Laboratory determination of leachable soil boron. Soil Sci. Soc. Am., Proc., 34: 871–875.

Rideal, E.K., 1930. Surface Chemistry. Cambridge University Press.

Selim, H.M. and Mansell, R.S., 1976. Analytical solution of the equation for transport of reactive solutes through soils. Water Resour. Res., 12: 528–532.

Swanson, R.A. and Dutt, G.R., 1973. Chemical and physical processes that affect atrazine movement and distribution in soil systems. Soil Sci. Soc. Am. Proc., 37: 872–876.

Tanji, K.K., 1970. A computer analysis on the leaching of boron from stratified soil columns. Soil Sci., 110: 44–51.

Turner, G.A., 1958. The flow-structure in packed beds. Chem. Eng. Sci., 7: 156–165.

Van de Pol, R.M., 1974. Solute Movement in a Layered Field Soil. MS thesis, New Mexico State University, Las Cruces, New Mexico.

Van Genuchten, M.Th., 1974. Mass Transfer Studies in Sorbing Porous Media, Ph.D. thesis, New Mexico State Univ., Las Cruces, New Mexico.

Van Genuchten, M.Th. and Wierenga, P.J., 1974. Simulation of one-dimensional solute transfer in porous media. New Mexico Agric. Exp. Sta. Bull., 628.

Van Genuchten, M.Th. and Wierenga, P.J., 1976a. Numerical solution for convective–dispersion with intra-aggregate diffusion and non-linear adsorption. In: G.C. van Steenkiste (Editor), System Simulation in Water Resources. North-Holland, Amsterdam.

Van Genuchten, M.Th. and Wierenga, P.J., 1976b. Mass transfer studies in sorbing porous media: I. Analytical solutions. Soil Sci. Soc. Am. J., 40: 473–480.

Van Genuchten, M.Th. and Wierenga, P.J., 1977. Mass transfer studies in sorbing porous media: II. Experimental evaluation with tritium (^3H_2O). Soil Sci. Soc. Am. J., 41: 272–278.

Van Genuchten, M.Th., Davidson, J.M. and Wierenga, P.J., 1974. An evaluation of kinetic and equilibrium equations for the prediction of pesticide movement through porous media. Soil Sci. Soc. Am. Proc., 38: 29–35.

Van Genuchten, M.Th., Wierenga, P.J. and O'Connor, G.A., 1977. Mass transfer studies in sorbing porous media: III. Experimental evaluation with 2,4,5-T. Soil Sci. Soc. Am. J., 41: 278–285.

Villermaux, J. and Van Swaay, W.P.M., 1969. Modèle représentatif de la distribution des temps de séjour dans un réacteur semi-infini à dispersion axiale avec zones stagnantes. Chem. Eng. Sci., 24: 1097—1111.

Warrick, A.W., Biggar, J.W. and Nielsen, D.R., 1971. Simultaneous solute and water transfer for an unsaturated soil. Water Resour. Res., 7: 1216—1225.

Wehner, J.F. and Wilhelm, R.H., 1956. Boundary conditions of flow reactor. Chem. Eng. Sci., 6: 89—93.

Wild, A., 1972. Nitrate leaching under bare fallow at a site in Northern Nigeria. J. Soil Sci., 23: 315—324.

Wild, A. and Babiker, I.A., 1976. The asymmetric leaching pattern of nitrate and chloride in a loamy sand under field conditions. J. Soil Sci., 27: 460—466.

Wood, A.L. and Davidson, J.M., 1975. Fluometuron and water content distribution during infiltration: measured and calculated. Soil Sci. Soc. Am. Proc., 39: 820—825.